

# Low-temperature absorption spectra and electron structure of $\text{HoFe}_3(\text{BO}_3)_4$ single crystal

A.V. Malakhovskii<sup>1</sup>, S.L. Gnatchenko<sup>2</sup>, I.S. Kachur<sup>2</sup>, V.G. Piryatinskaya<sup>2</sup>, and I.A. Gudim<sup>1</sup>

<sup>1</sup>*Kirensky Institute of Physics, 660036 Krasnoyarsk, Russian Federation*  
E-mail: malakha@iph.krasn.ru

<sup>2</sup>*B. Verkin Institute for Low Temperature Physics and Engineering,  
National Academy of Sciences of Ukraine, 61103 Kharkov, Ukraine*

Received May 23, 2016, published online March 24, 2017

Polarized absorption spectra of  $\text{HoFe}_3(\text{BO}_3)_4$  single crystal in the range of 8500–24500  $\text{cm}^{-1}$  were studied as a function of temperature beginning from 2 K. The ground and excited electron states of  $\text{Ho}^{3+}$  were identified. The abrupt changes of the spectra at the reorientation phase transition at 4.7 K were observed. The exchange splitting of some excited states were revealed and measured. They changed at the reorientation phase transition. Several vibronic transitions were observed. The splitting of absorption lines corresponding to the  $C_2$  local symmetry of the Ho ion was not observed. Moreover, spectra of some absorption bands correspond to splitting in the cubic crystal field. There are some absorption lines, whose polarization can not be explained both in  $D_3$  and  $C_2$  local symmetries. Some lines appear or disappear as a result of the transition from the easy axis to the easy plane state of the crystal. All these observations testify to the substantial changes of the local magnetic and structural properties in the excited states of the  $\text{Ho}^{3+}$  ion and to the strong influence of the magnetic moments orientation on the polarization of the electron transitions.

PACS: 78.40.Ha Absorption and reflection spectra: visible and ultraviolet, nonmetallic inorganics;  
71.70.-d Level splitting and interactions.

Keywords:  $f$ - $f$  transitions,  $\text{Ho}^{3+}$  ion, excited states, local properties.

## 1. Introduction

A number of the rare-earth ferrobates with the common formula  $\text{RFe}_3(\text{BO}_3)_4$  (where R is the rare-earth element) belong to the class of multiferroics — the materials which possess the interrelated magnetic, electric and elastic ordering (see, e.g., [1–7]). In recent years these compounds attract a growing interest in view of their manifold potential applications. A wide variety of magnetic properties of the ferrobates is conditioned by the coexistence and mutual influence of two magnetic subsystems: iron and rare-earth (RE).

Investigation of magnetic and magnetoelectric properties of the  $\text{HoFe}_3(\text{BO}_3)_4$  single crystal showed that it also refers to multiferroics [4–6]. In this crystal the considerable electric polarization in magnetic field [6], the giant magnetodielectric effect and the spontaneous polarization in the region of magnetic ordering [4] were found. It should be noted that the giant magnetoelectric polariza-

tion was also detected in alumoborate of holmium  $\text{HoFe}_3(\text{BO}_3)_4$  at the absence of magnetic ordering [8–10].

$\text{HoFe}_3(\text{BO}_3)_4$  crystal, as many of the ferrobates, undergoes the structural phase transition from  $R32$  to  $P3_121$  ( $D_3^4$ ) symmetry. The temperature of the transition depends strongly on the method of crystal growing: it amounts 427 K for the powder samples obtained by the solid-state synthesis [11] and 360 K for single crystals grown from a solution-melt [12]. Magnetic properties of  $\text{HoFe}_3(\text{BO}_3)_4$  were studied in Refs. 13, 14 and summarized and theoretically analyzed in Ref. 15. It was shown that the strong polarization effect of the Fe sublattice on the  $\text{Ho}^{3+}$  ions leads to the simultaneous ordering of both magnetic subsystems at  $T_N = 38$  K. The competition between the Fe and Ho anisotropies results in a spontaneous spin-reorientation phase transition from the easy plane to the easy axis state at  $T_{sr} = 4.7$  K. Neutron diffraction measurements [13] showed that in the both phases the magnetic structure is quite complicated and deviates from the collinear one. Later on the base of the resonant and

nonresonant x-ray scattering studies [16] it was supposed that in the easy-plane state magnetic moments of Ho form a basal plane spiral propagating along the  $C_3$  axis.

For the present, there are only few studies of optical spectra of  $\text{Ho}^{3+}$  ion in ferro- and aluminoborates. It should be noted a study of  $\text{Ho}^{3+}$ -doped  $\text{YAl}_3(\text{BO}_3)_4$  crystal in a wide spectral and temperature range [17], room temperature studies of  $\text{HoAl}_3(\text{BO}_3)_4$  [18] and the high-resolution spectroscopy of  $\text{HoFe}_3(\text{BO}_3)_4$  in the infrared region [12]. Up to now, there is no detailed spectroscopic studies of the holmium ferroborate in the visible region.

The subject of the present work is the low-temperature absorption spectrum of the  $\text{HoFe}_3(\text{BO}_3)_4$  single crystal and its transformation as a result of the spontaneous spin-reorientation phase transition. The special attention is given to selection rules and their correlation with the local symmetry of the  $\text{Ho}^{3+}$  ion.

## 2. Experimental details

$\text{HoFe}_3(\text{BO}_3)_4$  single crystals were grown from a bismuth trimolibdate solution-melt with a nonstoichiometric composition of the crystal forming oxides and with saturation temperature of  $T_{\text{sat}} \approx 960$  °C. The width of the metastable region was about 10–12 °C. Quasi-binary solution-melt formula was 75 mass % ( $\text{Bi}_2\text{Mo}_3\text{O}_{12} + 3\text{B}_2\text{O}_3 + 0.5\text{Ho}_2\text{O}_3$ ) + 25 mass %  $\text{HoFe}_3(\text{BO}_3)_4$ . In this solution-melt the trigonal  $\text{HoFe}_3(\text{BO}_3)_4$  was in the high-temperature phase and crystallized at least up to  $T \approx 900$  °C. The solution with a mass of 100 g was prepared in a platinum crucible. It was kept for 8–10 h at  $T = 1100$  °C for homogenization with permanent mixing by a reversibly rotating platinum rod. The crystals were grown on seeds. The temperature of the solution-melt was decreased to  $T = T_{\text{sat}} + 7$  °C. The platinum rod with four seeds of the size  $\sim 1 \text{ mm}^3$  was dipped into the solution, and rotation of rod with 30 revolutions per minute was switched on. After 10 min exposition the temperature was decreased to  $T = T_{\text{sat}} - 7$  °C. Further the temperature was lowered at a rate of 1–3 °C/24 h. The total duration of the crystal growth was 14 days. Isometric crystals with size about 7–10 mm were grown. For optical measurements a plate with the thickness of 85  $\mu$  was used.

The absorption spectra were measured with the light propagating normally to the  $C_3$  axis of the crystal for the light electric vector  $\mathbf{E}$  parallel (the  $\pi$  spectrum) and perpendicular (the  $\sigma$  spectrum) to the  $C_3$  axis. The spectral resolution was approximately equal to  $1.5 \text{ cm}^{-1}$ .

For the temperature measurements of absorption spectra a liquid-helium cooled cryostat was used. It had an internal volume filled by the gaseous helium where the sample was placed. Magnetic field was created by a superconducting solenoid with the Helmholtz type coils. The superconducting solenoid with the sample was placed in the liquid helium and measurements in the magnetic field were fulfilled at  $T = 2$  K.

## 3. Results and discussion

As mentioned, the  $\text{HoFe}_3(\text{BO}_3)_4$  crystal has structural phase transition from  $R32$  to  $P3_121$  ( $D_3^4$ ) symmetry above the room temperature [11]. At this transition, the local symmetry of RE ion decreases from  $D_3$  to  $C_2$  one. However, for the beginning we restrict ourselves to the  $D_3$  symmetry. Electron states in crystals of the axial symmetry have such characteristic as the crystal quantum number  $\mu$ . For the states with the integer momentum in trigonal crystals it has the values [19]:  $\mu = 0, +1, -1$ . Additionally, in the uniaxial crystals the electron states can be described in a first approximation by the  $|J, \pm M_J\rangle$  wave functions of the free atom. Between the values of  $\mu$  and  $M_J$  there is the following correspondence [19]:

$$M_J = 0 \pm 1 \pm 2 \quad (\pm 3)_{1,2} \quad \pm 4 \pm 5 \quad (\pm 6)_{1,2} \quad \pm 7 \pm 8 \quad (1)$$

$$\mu = 0 \pm 1 \mp 1 \quad 0 \quad \pm 1 \mp 1 \quad 0 \quad \pm 1 \mp 1 \quad (2)$$

$$A_1 \quad E \quad E \quad A_1, A_2 \quad E \quad E \quad A_1, A_2 \quad E \quad E \quad (3)$$

The corresponding irreducible representations in  $D_3$  symmetry are given in (3). In the  $|J, \pm M_J\rangle$  wave functions approximation, magnetic moment of the state is  $m = \mu_B g M_J$ , where  $g$  is the Landé factor of the free ion. The ground multiplet of the  $\text{Ho}^{3+}$  ion is  $^5I_8$  and, correspondingly,  $g = 1.25$ . According to Ref. 13, the  $\text{Ho}^{3+}$  ion in  $\text{HoFe}_3(\text{BO}_3)_4$  crystal has  $m = 5 \mu_B$  at  $T = 2$  K. Then  $M_J = 4$  but not 8 ( $m = 10 \mu_B$ ), as it was possible to expect, and the ground state has the  $E$  symmetry according to (1) and (3). In the same approximation the splitting of the  $\pm M_J$  doublet in magnetic field is

$$\Delta E = g_{CM} \mu_B H = 2g M_J \mu_B H = 2\mu_B H \frac{m}{\mu_B}. \quad (4)$$

Here  $g_{CM}$  is the Landé factor of the  $\pm M_J$  doublet in the  $|J, \pm M_J\rangle$  wave functions approximation. Thus,  $g_{CM} = 2g M_J = 10$ . According to [15] in the low-temperature easy-axis state the Fe–Ho exchange field is 25 kOe. Then from (4) we find the exchange splitting of the  $\text{Ho}^{3+}$  ion in the ground state in the  $|J, \pm M_J\rangle$  function approximation:  $\Delta E = 11.7 \text{ cm}^{-1}$ . Such value of the exchange splitting permits us to consider that at  $T = 2$  K only transitions from the lower component of the ground-state exchange splitting are observed.

At the conversion from a free atom to that in octahedron and further to the  $D_3$  symmetry position, the studied states of the  $\text{Ho}^{3+}$  ion are transformed in the following way:

$$J = 1 \rightarrow T_1 \rightarrow A_2 + E, \quad (5)$$

$$J = 2 \rightarrow E + T_2 \rightarrow E + (A_1 + E), \quad (6)$$

$$J = 3 \rightarrow A_2 + T_1 + T_2 \rightarrow A_2 + (A_2 + E) + (A_1 + E), \quad (7)$$

$$J = 4 \rightarrow A_1 + E + T_1 + T_2 \rightarrow A_1 + E + (A_2 + E) + (A_1 + E), \quad (8)$$

$$J = 5 \rightarrow E + 2T_1 + T_2 \rightarrow E + 2(A_2 + E) + (A_1 + E), \quad (9)$$

$$J = 6 \rightarrow A_1 + A_2 + E + T_1 + 2T_2 \rightarrow A_1 + A_2 + E + (A_2 + E) + 2(A_1 + E), \quad (10)$$

$$J = 8 \rightarrow A_1 + 2E + 2T_1 + 2T_2 \rightarrow A_1 + 2E + 2(A_2 + E) + 2(A_1 + E). \quad (11)$$

There is no total equivalence between presentations (1)–(3) and (5)–(11) for the splitting of states in crystals. The correspondence of one of them to the specific crystal depends on the strength of the uniaxial anisotropy. Only number of states and their degenerations are identical.

3.1. Transitions  ${}^5I_8 \rightarrow {}^5F_3$  (F band),  ${}^5F_2$  (G band),  ${}^3K_8$  (H band)

Let's begin from  ${}^5I_8 \rightarrow {}^5F_2$  (G) transition. Absorption spectrum of the G band consists of three lines (Figs. 1, 2), that corresponds to splitting of the  ${}^5F_2$  multiplet in  $D_3$  crystal field (6); the further splitting by  $C_2$  symmetry field is small and not observed. If the ground state has  $E$  symmetry, then, according to (6) and selection rules of Table 1, the absorption lines should have polarizations  $\pi\sigma$ ,  $\sigma$ ,  $\pi\sigma$ . If the ground state is  $A_1$  then they should have polarizations  $\sigma$ , 0,  $\sigma$  and polarizations  $\sigma$ ,  $\pi$ ,  $\sigma$  at  $A_2$  ground state. Comparing this with Figs. 1 and 2, we infer that the ground state has  $E$  symmetry in agreement with the above conclusion.

In the F and H bands (Figs. 1–3) mainly transitions into the  $E$  type states and in the separately standing  $A_2$  and  $A_1$  type states (F1 and H1 lines, respectively) are observed. Thus, even splitting due to the  $D_3$  crystal field is almost not observed, but only the splitting due to the cubic component of the crystal field occurs. However a small splitting of the F3 line (Figs. 2, 4) and some lines in the H band (Fig. 3) are noticeable. If the splitting of F3 line was due to  $A_1$  or  $A_2$  type

Table 1. Selection rules for electric dipole transitions in  $D_3$  symmetry

	$A_1$	$A_2$	$E$
$A_1$	–	$\pi$	$\sigma(\alpha)$
$A_2$	$\pi$	–	$\sigma(\alpha)$
$E$	$\sigma(\alpha)$	$\sigma(\alpha)$	$\pi, \sigma(\alpha)$

state, then the additional line would have  $\sigma$  polarization according to the selection rules of Table 1. However, both lines have  $\pi\sigma$  polarization, and we can suppose that the exchange splitting of the excited F3 state takes place. From Fig. 4 we find that this splitting is  $6 \text{ cm}^{-1}$ . Polarizations of additional lines in the H band correspond to  $A$  type states. A small splitting between  $E$  and  $A$  type states makes the (1)–(3) logic questionable. The observed spectra of the F and H bands are close to that in the cubic symmetry.

Absorption lines in the F and G bands practically do not shift as a result of the reorientation phase transition (see Figs. 1, 2) and only slightly shift in the H band. Absorption lines, appearing with the increasing temperature (Figs. 1, 2), permitted us to estimate positions of some of the lowest energy levels (Table 2). They were confirmed also by the spectra of another absorption bands. There are some transitions from excited states of the ground multiplet which have  $\pi$  polarization:  $F\pi$  and  $G\pi$  (Figs. 1, 2). Energies of these transitions correspond to transitions from the Gr4 and Gr5 states into the F2 and G2 states, respectively. The  $\pi$  polarization corresponds to  $A_1$ – $A_2$  transitions (Table 1). We could infer that the initial states are of the  $A$  symmetry. However, the excited states have  $(E+A)$  and  $E$  symmetries, respectively (Table 2). The discussed lines are observed after transition of the crystal into the easy-plane state. Therefore, it is possible to suppose that the unexpected polarizations are connected with the reorientation of the magnetization and (or) with the substantial change of the local symmetry in the corresponding excited states.

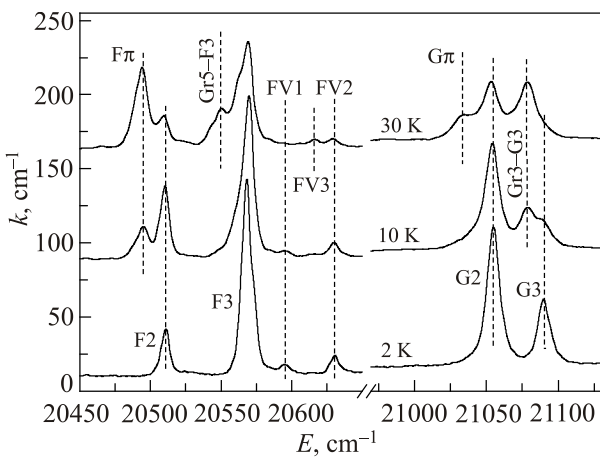


Fig. 1. Absorption spectra of transitions  ${}^5I_8 \rightarrow {}^5F_3$  (F band) and  ${}^5F_2$  (G band) in  $\pi$  polarization.

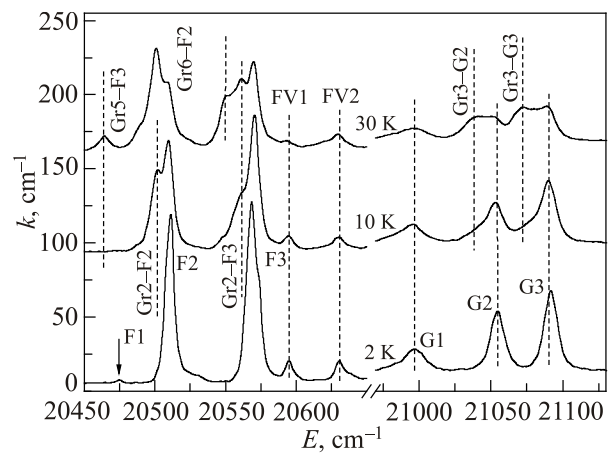


Fig. 2. Absorption spectra of transitions  ${}^5I_8 \rightarrow {}^5F_3$  (F band) and  ${}^5F_2$  (G band) in  $\sigma$  polarization.

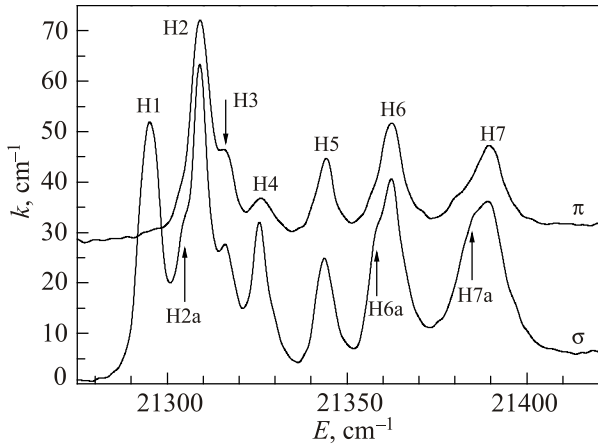


Fig. 3. Polarized absorption spectra of transition  ${}^5I_8 \rightarrow {}^3K_8$  (H band) at 2 K.

Vibronic states FV1 and FV2 (Figs. 1, 2) have  $E$  symmetry according to polarization of the corresponding absorption lines and selection rules of Table 1. Such vibronic states can be obtained in combination of F2 and F3 electron states of the  $E$  symmetry with any vibrations in the  $D_3$  local symmetry. On the basis of comparison with the data of infrared and Raman experiments [20,21], we infer that the vibronic states are repetitions of the electronic transition F2 by vibrations 84 and 120  $\text{cm}^{-1}$  of the  $E$  symmetry. Vibronic transition FV3 occurs from one of the lower excited states. Polarization of the vibronic transition FV3 (see Figs. 1, 2) corresponds to  $A_1$ – $A_2$  type transition according to Table 1. The vibronic state of the  $A$  type can be obtained in combination of the excited  $E$  state only with the  $E$  vibration:  $E \times E = A_1 + A_2 + E$ . Thus, FV3 is the transition from the Gr4 state (Table 2) to the vibronic state  $F2 + 120 \text{ cm}^{-1}$ . In Refs. 20, 21 the collective vibrations in the ground electron state were studied, while we deal with the local vibrations in the excited electron state. Therefore, some differences

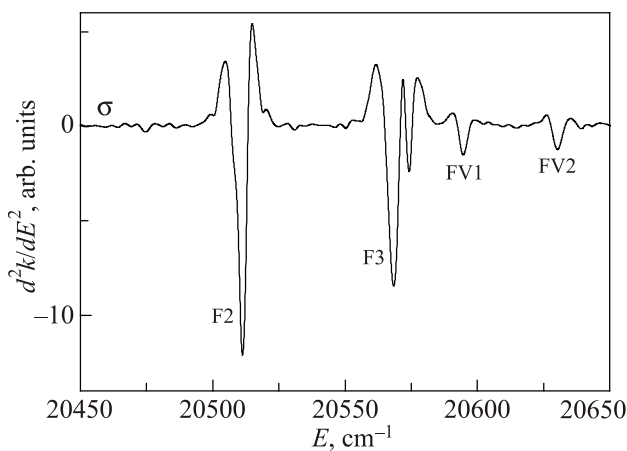


Fig. 4. The second derivative of the  $\sigma$ -polarized absorption spectrum of the  ${}^5I_8 \rightarrow {}^5F_3$  transition (F band) at 2 K.

Table 2. Parameters of transitions and states. Energies of transitions ( $E$ ) are given at 2 K.  $\Delta E_C$  and  $\Delta E_\perp$  are the exchange splitting in the easy-axis and easy-plane states, respectively

State	Level	$E, \text{cm}^{-1}$	Polarization	Symmetry	$\Delta E_C, \text{cm}^{-1}$	$\Delta E_\perp, \text{cm}^{-1}$	
${}^5I_8$	Gr1	0	–	$E$			
	Gr2	9	–	$A$			
	Gr3	12	–	$E$			
	Gr4	16	–	$A$			
	Gr5	21	–	$E$			
	Gr6	47	–	$A$			
	Gr7	58	–	$A_2$			
	Gr8	67	–	$A?$			
${}^5I_6$	A1	8604	$\pi, \sigma$				
	A2	8618	$\pi, \sigma$				
	A3	8649	$\pi, \sigma$				
	A4	8671	$\pi, \sigma$				
	A5	8686	$\pi, \sigma$				
	A6	8697	$\pi$				
	A7	8711	$\pi, \sigma$				
	A8	8722	$\pi, \sigma$				
${}^5I_5$	B1	11175	$\pi, \sigma$	$E$			
	B2	11195	$\sigma$	$A$			
	B3	11217	$\sigma$	$A$			
	B4	11238	$\pi, \sigma$	$E$			
	B5	11245	$\sigma$	$A$			
	B6a	11258	$\pi, \sigma$	$E$	5		
	B6b	11263	$\pi, \sigma$	$E$			
B7	11273	$\pi, \sigma$	$E$				
${}^5F_5$	D1	15403	$\sigma$	$A_1?$			
	D2	15423	$\pi, \sigma$	$E$			
	D3	15434	$\pi, \sigma$	$E$			
	D4	15449	$\pi, \sigma$	$E$			
	D5	15482	$\sigma$	$A$			
	D6	15510	$\sigma$	$A$			
	D7	15568	$\pi, \sigma$	$E$			
${}^5S_2$	E1	18392	$\sigma$	$A_1$			
	E2	18399	$\pi, \sigma$	$E$			
	E3	18416	$\pi, \sigma$	$E$			
	${}^5F_4$	E4	18502	$\pi, \sigma$	$E$		
		E5	18507	$\sigma$	$A$		
		E6	18526	$\pi, \sigma$	$E$	6	0
		E6a	18532	$\pi, \sigma$	$E$		
		E7	18563	$\sigma$	$A$		
		E8	18582	$\pi$	?		
E9		18592	$\pi, \sigma$	$E$			
${}^5F_3$		F1	20474	$\sigma$	$A_2$		
		F2	20511	$\pi, \sigma$	$E + A$	6	
	F3	20568	$\pi, \sigma$	$E + A$			
	FV1	20595	$\pi, \sigma$	$E$			
	FV2	20631	$\pi, \sigma$	$E$			

State	Level	$E, \text{cm}^{-1}$	Polarization	Symmetry	$\Delta E_C, \text{cm}^{-1}$	$\Delta E_L, \text{cm}^{-1}$
$^5F_2$	G1	20997	$\sigma$	$A_1$		
	G2	21055	$\pi, \sigma$	$E$		
	G3	21090	$\pi, \sigma$	$E$		
$^3K_8$	H1	21295	$\sigma$	$A_1$		
	H2a	21304	$\sigma$	$A$		
	H2	21309	$\pi, \sigma$	$E$		
	H3	21316	$\pi, \sigma$	$E$		
	H4	21325	$\pi, \sigma$	$E + A$		
	H5	21344	$\pi, \sigma$	$E$		
	H6a	21358	$\sigma$	$A$		
	H6	21362	$\pi, \sigma$	$E$		
	H7a	21385	$\sigma$	$A$		
	H7	21389	$\pi, \sigma$	$E$		
$^5G_6+$ $^5F_1$	I1	21968	$\sigma$	$A$	4.8	10.7
	I2	21986	$\sigma$	$A$		
	I3	22014	$\pi, \sigma$	$E$		
	I4	22054	$\pi, \sigma$	$E$		
	I5	22074	$\sigma$	$A$		
	I6	22094	$\pi, \sigma$	$E$	8	
	I7	22178	$\pi, \sigma$	$E$		
	I8	22202	$\sigma$	$A$		
	I9	22224	$\pi, \sigma$	$E$		
	I10	22238	$\sigma (?)$	$A$		
	I11	22292	$\sigma$	$A$		
$^5G_5$	J1	23844	$\pi, \sigma$		5.0	4.6
	J2	23866	$\pi, \sigma$			
	J3	23897	$\pi, \sigma$			
	J4	23914	$\pi, \sigma$			
	J5	23950	$\pi, \sigma$			
	J6	23966	$\pi, \sigma$			
	J7	24007	$\pi, \sigma$			

between energies of the vibrations obtained in the Raman, IR and optical experiments are possible.

### 3.2. Transitions $^5I_8 \rightarrow ^5F_5$ (D band), $^5I_5$ (B band) and $^5G_5$ (J band)

Excited states of these transitions have  $J = 5$ . Majority of lines of the D band, except Da and Db ones (Fig. 5), are easily identified at  $T = 2$  K in the  $D_3$  symmetry approximation (Table 2) basing on their polarizations, and they correspond to the total (9) decomposition. The Da and Db lines are, probably, the exciton-magnon ones (magnon in the Fe sublattice), at least the Db line, whose distance of  $23.7 \text{ cm}^{-1}$  from the D7 line is equivalent to 34 K. Indeed, a peak of the two-magnon Raman scattering was observed at approximately  $52 \text{ cm}^{-1}$  in some ferrobates [22]. The Da line can be also the consequence of the D2 line exchange splitting.

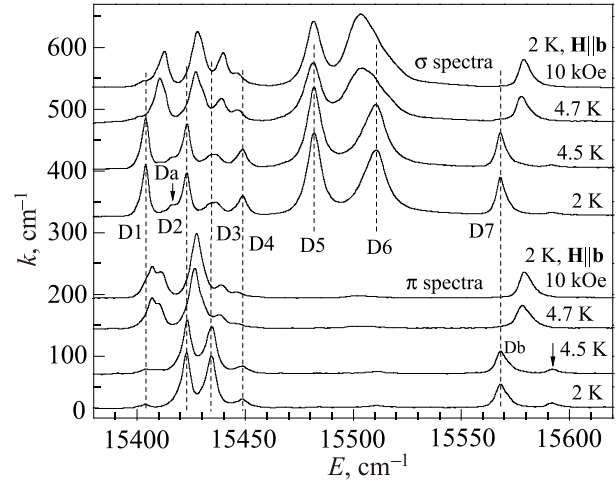


Fig. 5. Polarized absorption spectra of the  $^5I_8 \rightarrow ^5F_3$  transition (D band).

As a result of the spin-reorientation transition at 4.7 K all transitions (except D5) shift in different directions (Fig. 5). These shifts reflect both changes of energies of the ground and excited states which can not be separated. Appearance of the D1 line in  $\pi$  polarization and the splitting of the D1 and D6 lines after transition to the easy-plane state (Fig. 5) are unexpected phenomena since D1 and D6 states are singlets. The only possible assumption is that, first, two nonequivalent positions of the  $\text{Ho}^{3+}$  ions appear in the D1 and D6 excited states and, second, polarization of transitions into these states is mainly governed by the Ho magnetic moment orientation rather than by the crystal environment. In Fig. 5 there are also spectra at  $T = 2$  K in the magnetic field  $\mathbf{H} \parallel \mathbf{b}$  just after the spin-reorientation transition to the same easy-plane state as that at 4.7 K without the magnetic field [15]. These spectra are practically identical to those after the temperature-induced reorientation transition (Fig. 5). Thus, the spectra are totally defined by the Ho magnetic moment orientation. According to [15], the easy-plane state in  $\mathbf{H} \parallel \mathbf{b}$  is the one domain state. Consequently, the observed splitting of the D1 and D6 states can not be connected with the difference of the  $\text{Ho}^{3+}$  states in domains and domain walls. Indeed, increase of the magnetic field  $\mathbf{H} \parallel \mathbf{b}$  does not eliminate the splitting of the states. The nonequivalent positions can be referred to the inverse twins on the one hand and to the boundaries between them on the other hand. Additionally, the unusual behavior of the D1 line polarization testifies to the strong change of the local symmetry in the D1 electron state in the easy-plane state of the crystal. Figure 6 demonstrates transformation of the  $\pi$ -polarized spectrum of the D7 line in the region of the spin-reorientation transition. These spectra testify that in some temperature range two magnetic phases coexist.

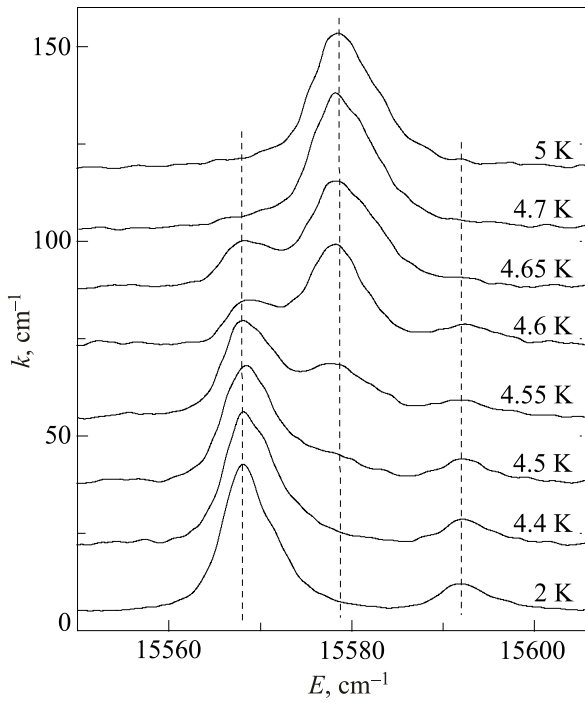


Fig. 6. Temperature variation of a fragment of the  $\pi$ -polarized absorption spectrum of the  ${}^5I_8 \rightarrow {}^5F_5$  transition (*D* band).

The reorientation transition at 4.7 K weakly influences the B band spectrum (see Fig. 7). The absorption lines are mainly identified in the  $D_3$  local symmetry approximation (Table 2). The B2 line has a weak  $\pi$  polarization, however there is no other possible identification than that given in Table 2. The splitting of the B6 line is probably the exchange splitting (Table 2).

Number of lines in the absorption spectrum of the J band (Fig. 8) corresponds to the splitting in the  $D_3$  symmetry but their polarizations do not correspond to this symmetry. In particular, there are no purely  $\sigma$ -polarized lines corresponding to  $E \rightarrow A$  type transitions

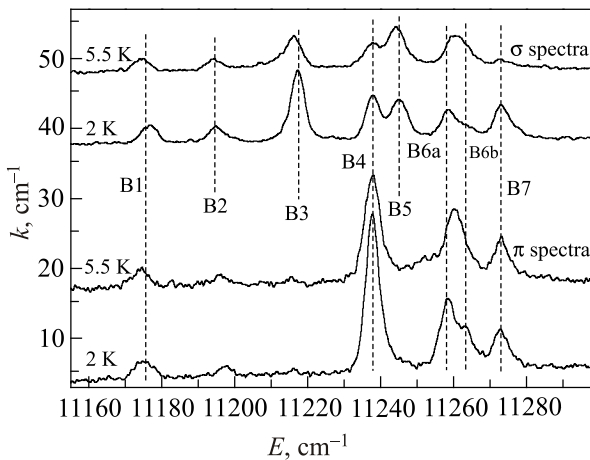


Fig. 7. Polarized absorption spectra of the  ${}^5I_8 \rightarrow {}^5I_5$  transition (*B* band).

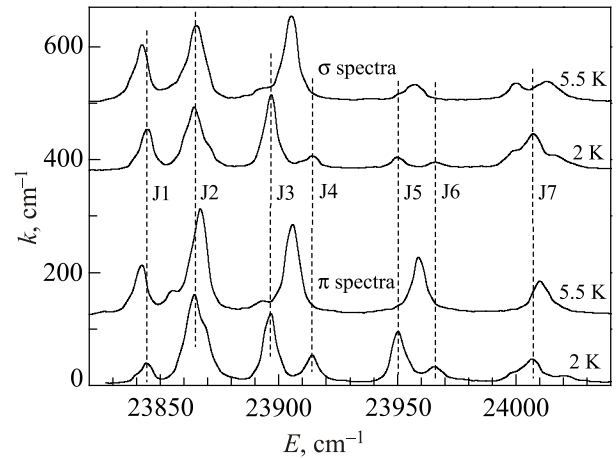


Fig. 8. Polarized absorption spectra of the  ${}^5I_8 \rightarrow {}^5G_5$  transition (*J* band).

(see Table 1). This is one more indication of the changes of the local properties in the excited states. After transition into the easy-plane state some lines shift and J4 and J6 lines disappear. The J7 line is split into three components, probably due to the crystal field and exchange interaction. The J2 line is split by the exchange field. In the easy-axis state the splitting is a little larger than that in the easy-plane state (Table 2).

### 3.3. Transition ${}^5I_8 \rightarrow {}^5I_6$ (*A* band)

Absorption spectra of this band (Fig. 9) contain 8 lines, while according to (10) there should be 9 lines. Moreover, there should be 5  $\sigma$ -polarized lines corresponding to transitions from the *E* type into the *A* type states (see (10)). A6 line has practically  $\pi$  polarization that corresponds to the  $A_1 \leftrightarrow A_2$  transitions (Table 1). Thus, symmetries of the excited states of the *A* band can not be identified that testifies to the specific local properties in the excited states.

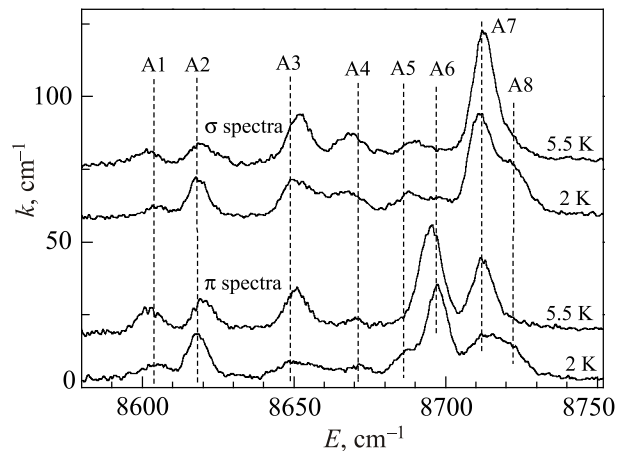


Fig. 9. Polarized absorption spectra of the  ${}^5I_8 \rightarrow {}^5I_6$  transition (*A* band).

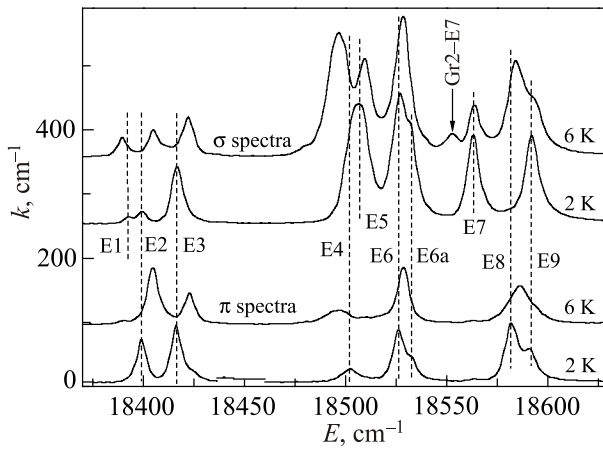


Fig. 10. Polarized absorption spectra of the  ${}^5I_8 \rightarrow {}^5S_2 + {}^5F_4$  transitions (E band).

### 3.4. Transition ${}^5I_8 \rightarrow {}^5S_2 + {}^5F_4$ (E band)

The states  ${}^5S_2$  and  ${}^5F_4$  are good separated in these spectra (Fig. 10) and their polarizations mainly correspond to the splitting (6), (8) and to the selection rules of Table 1. The E8 line is an exception. It should have the  $\sigma$  polarization, corresponding to the  $E \rightarrow A$  type transition, but it has  $\pi$  polarization corresponding to  $A_1 \leftrightarrow A_2$  type transition. However it acquires the  $\sigma$  polarization in the easy-plane state (Fig. 10). Rather substantial shifts of lines are observed as a result of the reorientation transition (Fig. 10). The E6 line demonstrates the exchange splitting in the easy-axis state which disappears in the easy-plane state (Fig. 10, Table 2).

### 3.5. Transition ${}^5I_8 \rightarrow {}^5G_6 + {}^5F_1$ (I band)

Number and polarizations of lines in this band correspond to the splitting in the  $D_3$  symmetry according to (5), (10) and Table 1, but it is impossible to separate  ${}^5G_6$  and  ${}^5F_1$  states (Fig. 11). The I3 state splits in the exchange field of the iron.

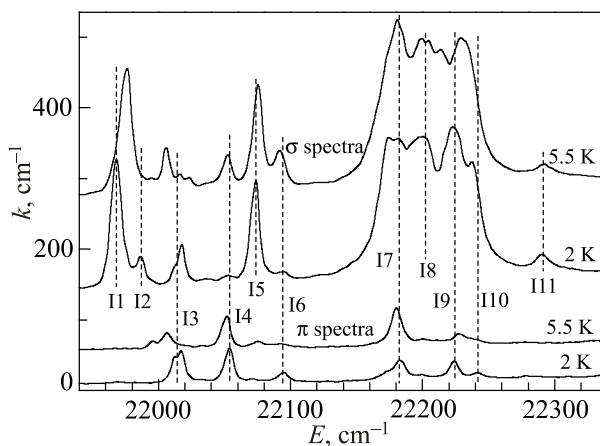


Fig. 11. Polarized absorption spectra of the  ${}^5I_8 \rightarrow {}^5G_6 + {}^5F_1$  transitions (I band).

This splitting substantially changes as a result of the reorientation transition in the crystal (Fig. 11 and Table 2). The I1 and I3 lines appreciably shift in opposite directions as a result of the reorientation transition. The I2 line disappears but the I4 and I6 lines strongly increase in the  $\sigma$  polarization after transition into the easy-plane state (Fig. 11).

## 4. Conclusions

Polarized absorption spectra of  $\text{HoFe}_3(\text{BO}_3)_4$  in the range of  $8500\text{--}24500\text{ cm}^{-1}$  were studied as a function of temperature beginning from 2 K. The threshold changes of positions and intensities of some absorption lines at the reorientation phase transition at 4.7 K were observed. Several vibronic transitions were observed, which correspond to the local vibrations in one of the excited states. Energies of the lowest states of the ground multiplet were found (Table 2). They rather well correspond to those given in Ref. 23, but appreciably diverge from those given in Ref. 15. The exchange splitting of some (but not all) excited states were revealed and measured. They changed at the reorientation phase transition. Basing on the Ref. 15 data, the exchange splitting of the ground state was estimated in the  $|J, \pm M_J\rangle$  wave function approximation as being equal to  $11.7\text{ cm}^{-1}$ . It was not measured experimentally since transitions from the upper component of the ground-state exchange splitting were not observed. Similar phenomenon was earlier took place in the  $\text{Nd}_{0.5}\text{Gd}_{0.5}\text{Fe}_3(\text{BO}_3)_4$  crystal: only some transitions of such kind were observed [24].

The crystal field splitting of states revealed a number of peculiarities. In particular, the splitting corresponding to the  $C_2$  local symmetry of the Ho ion was not observed. Moreover, spectra of some absorption bands correspond to splitting in the cubic crystal field. Description of states in terms of the  $|J, \pm M_J\rangle$  wave functions was found to be not enough suitable for the studied crystal in contrast to some other crystals with the axial symmetry such as, e.g.,  $\text{TbFe}_3(\text{BO}_3)_4$  [25]. This is, apparently, connected with the weak axial anisotropy of the  $\text{Ho}^{3+}$  ion that reveals also in a very low temperature of the reorientation phase transition to the easy-axis state. There are some absorption lines, whose polarization can not be explained both in  $D_3$  and  $C_2$  local symmetries. Some lines appear or disappear as a result of the transition from the easy axis to the easy-plane state of the crystal. All these observations testify to the substantial changes of the local magnetic and structural properties in the excited states of the  $\text{Ho}^{3+}$  ion and to the strong influence of the magnetic moments orientation on the polarization of the electron transitions. In the easy-plane state the crystal actually loses axial symmetry.

## Acknowledgments

The work was supported by the Russian Foundation for Basic Researches grant 16-02-00273 and by the President of Russia grant No. Nsh-7559.2016.2.

1. A.K. Zvezdin, S.S. Krotov, A.M. Kadomtseva, G.P. Vorob'ev, Yu.F. Popov, A.P. Pyatakov, L.N. Bezmaternykh, and E.A. Popova, *Pis'ma v ZhETF* **81**, 335 (2005) [*JETP Lett.* **81**, 272 (2005)].
2. A.K. Zvezdin, G.P. Vorob'ev, A.M. Kadomtseva, Yu.F. Popov, A.P. Pyatakov, L.N. Bezmaternykh, A.V. Kuvardin, and E.A. Popova, *Pis'ma v ZhETF* **83**, 600 (2006) [*JETP Lett.* **83**, 509 (2006)].
3. F. Yen, B. Lorenz, Y.Y. Sun, C.W. Chu, L.N. Bezmaternykh, and A.N. Vasiliev, *Phys. Rev. B* **73**, 054435 (2006).
4. R.P. Chaudhury, F. Yen, B. Lorenz, Y.Y. Sun, L.N. Bezmaternykh, V.L. Temerov, and C.W. Chu, *Phys. Rev. B* **80**, 104424 (2009).
5. A.M. Kadomtseva, Yu.F. Popov, G.P. Vorob'ev, A.P. Pyatakov, S.S. Krotov, P.I. Kamilov, V.Yu. Ivanov, A.A. Mukhin, A.K. Zvezdin, L.N. Bezmaternykh, I.A. Gudim, and V.L. Temerov, *Fiz. Nizk. Temp.* **36**, 640 (2010) [*Low Temp. Phys.* **36**, 511 (2010)].
6. A.M. Kadomtseva, G.P. Vorob'ev, Yu.F. Popov, A.P. Pyatakov, A.A. Mukhin, V.Yu. Ivanov, A.K. Zvezdin, I.A. Gudim, V.L. Temerov, and L.N. Bezmaternykh, *ZhETF* **141**, 930 (2012) [*JETP* **114**, 810 (2012)].
7. A.L. Freidman, A.D. Balaev, A.A. Dubrovskii, E.V. Eremin, K.A. Shaikhutdinov, V.L. Temerov, and I.A. Gudim, *Fiz. Tverd. Tela* **57**, 1334 (2015) [*Phys. Solid State* **57**, 1357 (2015)].
8. K.-C. Liang, R.P. Chaudhury, B. Lorenz, Y.Y. Sun, L.N. Bezmaternykh, V.L. Temerov, and C.W. Chu, *Phys. Rev. B* **83**, 180417(R) (2011).
9. A.I. Begunov, A.A. Demidov, I.A. Gudim, and E.V. Eremin, *Pis'ma v ZhETF* **97**, 611 (2013) [*JETP Lett.* **97**, 528 (2013)].
10. A.L. Freydmán, A.D. Balaev, A.A. Dubrovskiy, E.V. Eremin, V.L. Temerov, and I.A. Gudim, *J. Appl. Phys.* **115**, 174103 (2014).
11. Y. Hinatsu, Y. Doi, K. Ito, M. Wakeshima, and A. Alemi, *J. Solid State Chem.* **172**, 438 (2003).
12. D.A. Erofeev, E.P. Chukalina, L.N. Bezmaternykh, I.A. Gudim, and M.N. Popova, *Optika i Spektroskopiya* **120**, 59 (2016).
13. C. Ritter, A. Vorotynov, A. Pankrats, G. Petrakovskii, V. Temerov, I. Gudim, and R. Szymczak, *J. Phys.: Condens. Matter* **20**, 365209 (2008).
14. A. Pankrats, G. Petrakovskii, A. Kartashev, E. Eremin, and V. Temerov, *J. Phys.: Condens. Matter* **21**, 436001 (2009).
15. A.A. Demidov and D.V. Volkov, *Fiz. Tverd. Tela* **53**, 925 (2011) [*Phys. Solid State* **53**, 985 (2011)].
16. D.K. Shukla, S. Francoual, A. Skaugen, M. v. Zimmermann, H.C. Walker, L.N. Bezmaternykh, I.A. Gudim, V.L. Temerov, and J. Stempfer, *Phys. Rev. B* **86**, 224421 (2012).
17. A. Baraldi, R. Capelletti, M. Mazzerà, N. Magnani, I. Földvári, and E. Beregi, *Phys. Rev. B* **76**, 165130 (2007).
18. D.A. Ikonnikov, A.V. Malakhovskii, A.L. Sukhachev, V.L. Temerov, A.S. Krylov, A.F. Bovina, and A.S. Aleksandrovsky, *Opt. Mater.* **37**, 257 (2014).
19. M.A. El'yashevitch, *Spectra of Rare-Earths*, Gosteh-teorizdat, Moscow (1953) (in Russian).
20. V.I. Zinenko, M.S. Pavlovskii, A.S. Krylov, I.A. Gudim, and E.V. Eremin, *ZhETF* **144**, 1174 (2013) [*J. Exp. Theor. Phys.* **117**, 1032 (2013)].
21. S.N. Sofronova, Yu.V. Gerasimova, A.N. Vtyurina, I.A. Gudim, N.P. Shestakov, and A.A. Ivanenko, *Vibrational Spectroscopy* **72**, 20 (2014).
22. D. Fausti, A.A. Nugroho, P.H.M. van Loosdrecht, S.A. Klimin, M.N. Popova, and L.N. Bezmaternykh, *Phys. Rev. B* **74**, 024403 (2006).
23. E.P. Chukalina, T.N. Stanislavchuk, M.N. Popova, B.Z. Malkin, L.N. Bezmaternykh, and I.A. Gudim, in *Proceedings of the XXI International Conference "New in Magnetism and Magnetic Materials" (NMMM), Moscow, Russia, June 28–July 4 (2009)*, p. 510.
24. A.V. Malakhovskii, S.L. Gnatchenko, I.S. Kachur, V.G. Piryatinskaya, and V.L. Temerov, *Opt. Mater.* **52**, 126 (2016).
25. A.V. Malakhovskii, S.L. Gnatchenko, I.S. Kachur, V.G. Piryatinskaya, A.L. Sukhachev, and V.L. Temerov, *Eur. Phys. J. B* **80**, 1 (2011).